



HAL
open science

Optimal virtual sources distribution in 3-D diverging wave Ultrasound Imaging: an experimental study

P. Mattesini, G. Le Moign, E. Roux, E. Badescu, L. Petrusca, O. Basset, P. Tortoli, H. Liebgott

► To cite this version:

P. Mattesini, G. Le Moign, E. Roux, E. Badescu, L. Petrusca, et al.. Optimal virtual sources distribution in 3-D diverging wave Ultrasound Imaging: an experimental study. IEEE International Ultrasonics Symposium, Oct 2018, Kobe, Japan. 10.1109/ULTSYM.2018.8579668 . hal-01955120

HAL Id: hal-01955120

<https://hal.science/hal-01955120>

Submitted on 24 Mar 2019

HAL is a multi-disciplinary open access archive for the deposit and dissemination of scientific research documents, whether they are published or not. The documents may come from teaching and research institutions in France or abroad, or from public or private research centers.

L'archive ouverte pluridisciplinaire **HAL**, est destinée au dépôt et à la diffusion de documents scientifiques de niveau recherche, publiés ou non, émanant des établissements d'enseignement et de recherche français ou étrangers, des laboratoires publics ou privés.

Optimal virtual sources distribution in 3-D Diverging Wave Ultrasound Imaging: an experimental study

Paolo Mattesini*, Goulven Le Moign^{†‡}, Emmanuel Roux[†], Émilie Badescu[†], Lorena Petrusca[†], Olivier Basset[†], Piero Tortoli* and Hervé Liebgott[†]

* Department of Information Engineering, Università Degli Studi di Firenze, Firenze, Italy

[†] CREATIS, Univ.Lyon, INSA-Lyon, UCBL1, CNRS UMR 5220, Inserm U1206, UJM-Saint Etienne, 69100, Villeurbanne, France

[‡] GAUS, Dept. Mechanical Engineering, Université de Sherbrooke, Sherbrooke, QC, Canada J1K 2R1

e-mail: paolo.mattesini@unifi.it

Abstract—The use of 2-D array probes to perform 3-D ultrasound imaging is still investigated in many domains. The extension from 2-D to 3-D imaging causes problems because of the need to control a very large number of elements on the probe. It might be overcome by using 2-D sparse array. This problem has been recently shown that sparse 2-D arrays can be used for 3-D fast ultrasound imaging based on the transmission of Diverging Waves (DW). The aim of this work is to experimentally analyze how the distribution of a given number (25) of Virtual Sources (VS) over a predefined area affects the images obtained with one fully populated probe and two sparse array probes, respectively. In order to do that, gridded and spiral distributions of virtual sources have been implemented. The results show that with the spiral distribution there is a general improvement of the contrast despite of a degradation on both lateral and axial resolutions.

Index Terms—3-D Ultrasound imaging, 2-D Sparse array, Diverging waves, Virtual sources.

I. INTRODUCTION

3-D real-time ultrasound imaging by using 2-D array probe is still widely investigated in both academic and industrial domain [1]–[3]. In the medical field, 3-D ultra-fast imaging is also studied because of its interest in cardiac applications [4]–[7] such as for heart strain estimation. However, it is currently not possible to acquire volumetric data at adequate temporal and spatial resolution in a single heartbeat on current clinical scanners [8], because of the huge amount of channels that a fully populated probe would request.

Several strategies have been studied to reduce this number of channels. On one hand, techniques based on addressing a large number of active elements while reducing the number of channels include: micro-beamforming [9]–[17], row-column addressing [17]–[23] and channel multiplexing [24]. Each one promises good results but leads to a lack of control on the individual elements and reduces the flexibility. On the other hand, sparse array [25]–[30] can be designed to fix the number of elements, individually controlled by an equal number of

channels, to match with up-to-date scanners. This approach may be used to have a full control of the transmitted waves despite of Signal-to-Noise Ratio (SNR) and contrast losses.

In previous studies [31], [32], it has been experimentally demonstrated that sparse 2-D arrays can be used for implementing fast volumetric ultrasound imaging based on the transmission (TX) of Diverging Waves (DWs). With any kind of 2-D arrays (sparse or fully populated) the ideal location of virtual sources (VS) for DWs is still undefined.

The aim of this work is to experimentally analyze how the VS distribution affects the images obtained with a reference 2-D array, a random 256 elements sparse array and a 256 elements sparse array initially optimized for focused transmission [25], [31], [33].

II. METHODS

A. Probes configuration

A 32×32 elements 2-D array probe (VermonTM, Tours, France) was connected to four synchronized Vantage-256 research scanners (VerasonicsTM, Inc., Kirkland, WA, USA). Once they were synchronized, up to 1024 elements of the array may be monitored [34]. The piezoelectric elements have a 3 MHz center frequency and the Vantage-256 works at 12 MHz sampling frequency.

Three configurations have been established (Fig. 1): the fully populated probe using all the 32×32 elements (`Ref1024`) which acts as a reference, a group of 256 elements randomly selected among the 1024 (`rand256`) and the optimized version (`opti256`) using 256 elements selected according to an algorithm optimized for focused wave transmission.

B. Diverging Waves and Coherent Compounding

Each image was computed using a standard beamforming technique. The term “Virtual Source” (VS) refers to the position of a point source producing a desired diverging wave. Each VS produces one image. Such waves cover proper

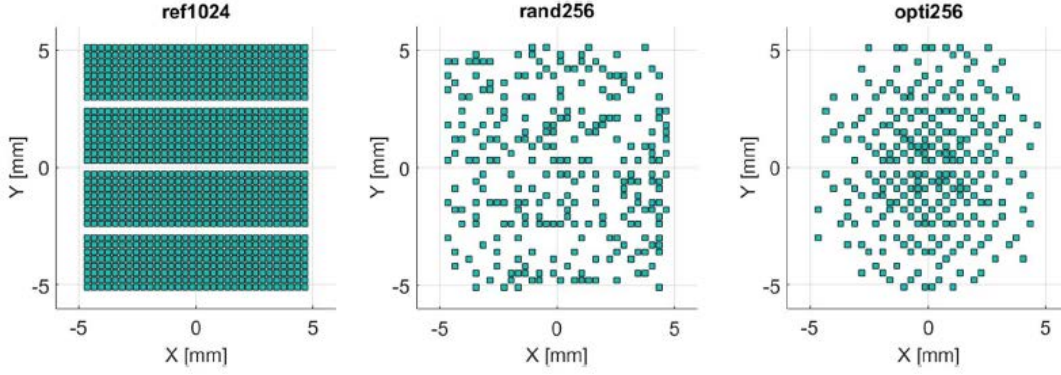


Fig. 1: Probes used: fully populated (ref1024), random generation of 256 elements (rand256) and random 256 elements optimized (opti256) [32]

volume, as necessary in echocardiography to cover the heart and “pass” trough at probe, whose dimension cannot be too large with respect to the human intercostal space, as requested by the clinicians.

By making several radiofrequency, from different virtual sources, an improved image can be obtained after a coherent summation of all of them. This coherent compounding [4], [35] takes advantage of constructive and destructive interferences (speckle) present in ultrasound images to smooth the resulting image while preserving the acoustic contrast.

C. Virtual Sources Distribution

The set of VS can be seen as a virtual probe. Two VS positioning strategies have been considered (Fig 2): distributed on a regular grid and on a spiral grid, with the aim of increasing the SNR and reducing grating lobes of the virtual probe. In both cases, the VS were located at $r = 25$ mm or $r = 40$ mm from the 2-D array center, with angle ranges of 60° or 120° . The number of VS was set to 25 in all configurations.

D. Phantom and Evaluation Criteria

The images were performed on a Gammex™ (Sono410 SCG) or a CIRS™ (054GS) phantom. The performance metrics include the lateral and axial Full Width at Half Maximum (FWHM), Contrast Ratio (CR) and Contrast to Noise Ratio (CNR) as follow:

$$\text{CR} = 20 \log_{10} \left(\frac{|\mu_{\text{bck}} - \mu_{\text{cyst}}|}{\sqrt{\mu_{\text{bck}}^2 + \mu_{\text{cyst}}^2}} \right), \quad (1)$$

$$\text{CNR} = 20 \log_{10} \left(\frac{|\mu_{\text{bck}} - \mu_{\text{cyst}}|}{\sqrt{\sigma_{\text{bck}}^2 + \sigma_{\text{cyst}}^2}} \right), \quad (2)$$

where μ_{area} and σ_{area} are the respective mean and standard deviation of the beamformed signal envelope (before log-compression) values on the background (bck) and inside a cyst (cyst).

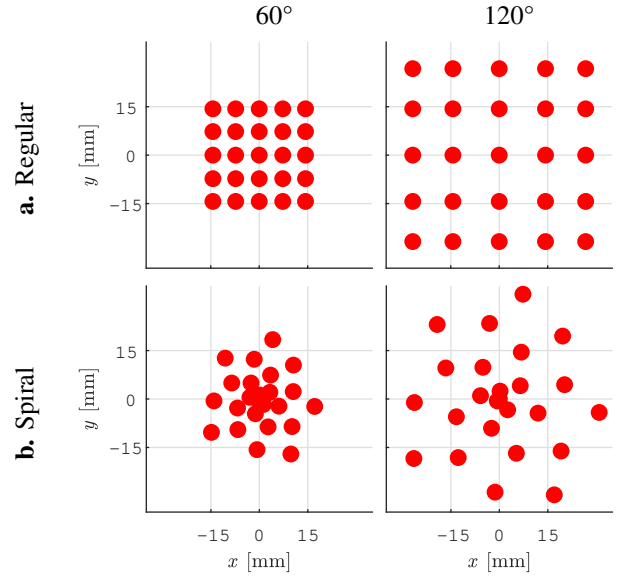


Fig. 2: Virtual sources distribution strategies

III. RESULTS

The resulting images in the xz plan are shown in Fig. 3 for $r = 40$ mm, the resolution and contrast measurement are also shown in Table I.

In Ref1024, a general improvement of CR and CNR is obtained by using the spiral VS distribution rather than a regular one. The axial resolution remains the same while the lateral resolution is worse (up to 0.4 mm coarser). For Opti256 the trend is similar: CR and CNR are better with the spiral VS distribution but both resolutions are worse (up to 0.3 mm coarser for the lateral and up to 0.1 mm for the axial). In Rand256 the results are similar to Opti256: the spiral VS distribution gives better CR and CNR but worse resolution (up to 0.4 mm coarser for the lateral and up to 0.2 mm for the axial). Table I provides an overall comparison among all the 3 probe configurations. Results suggest that, compared to a gridded VS distribution, a spiral one increases

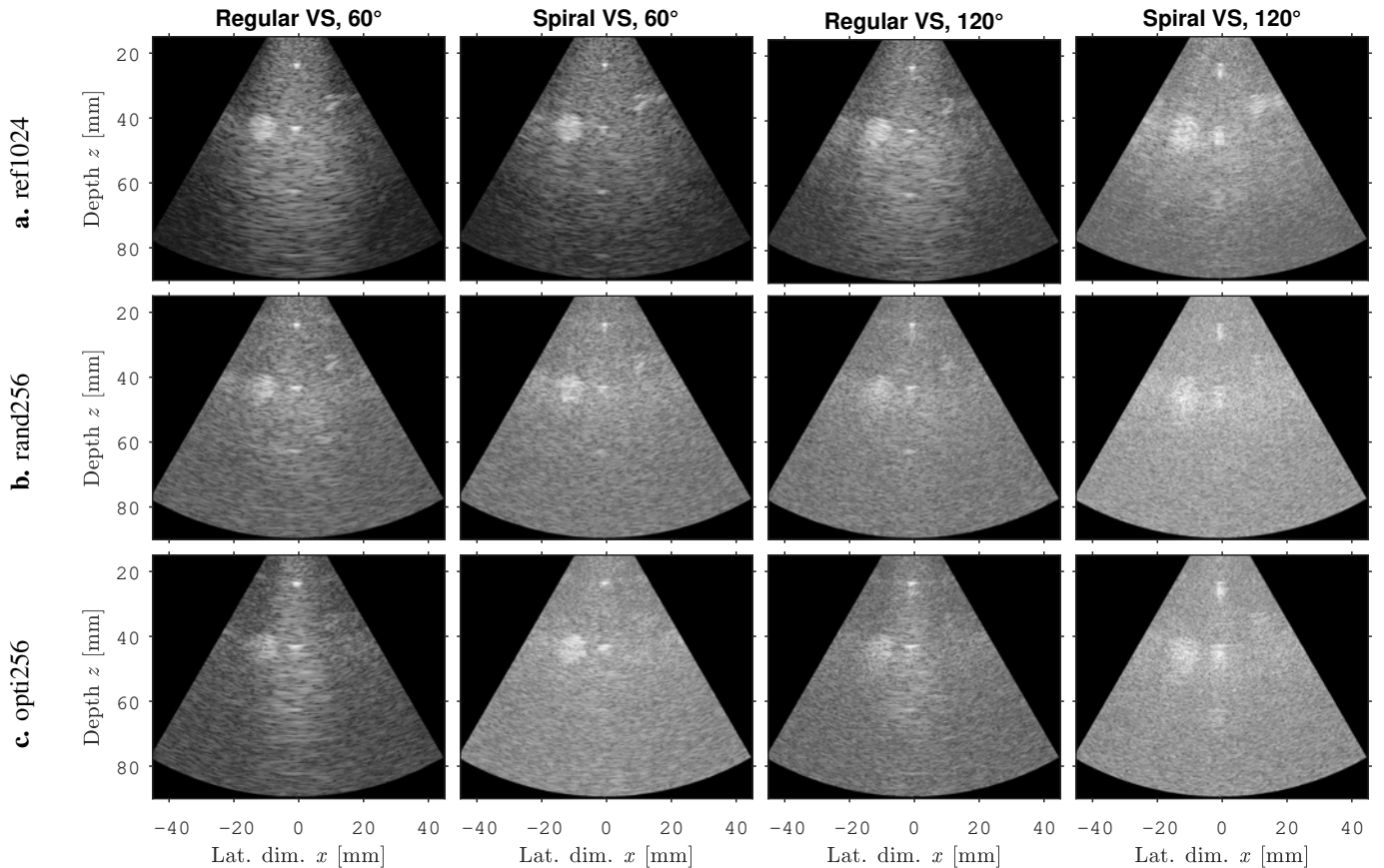


Fig. 3: Compounded images with experimental data acquired with 25 VS on 40 mm, on the Gammex™ phantom. The dynamic is set to 60 dB

TABLE I: Results for $r = 40$ mm

| REF1024 VSs d. 40 mm | | | | |
|----------------------|------------------------|-----------------------|------------|-------------|
| | Mean Lat. Res. [mm] | Mean Ax. Res. [mm] | CR [dB] | CNR [dB] |
| Grid 60° | 1.98 | 0.47 | -8.8 | -10.2 |
| Grid 120° | 2.13 | 0.44 | -2.3 | -10.2 |
| Spiral 60° | 2.39 | 0.47 | -11.5 | -8.8 |
| Spiral 120° | 2.29 | 0.45 | -6.4 | -11.0 |
| Rand256 VSs d. 40 mm | | | | |
| Grid 60° | 2.06 | 0.45 | -3.0 | -16.2 |
| Grid 120° | 2.06 | 0.58 | 0.4 | -31.0 |
| Spiral 60° | 2.46 | 0.67 | -5.5 | -12.7 |
| Spiral 120° | 2.49 | 0.75 | -1.1 | -24.7 |
| Opti256 VSs d. 40 mm | | | | |
| Grid 60° | 3.11 | 0.44 | -2.5 | -17.5 |
| Grid 120° | 2.78 | 0.49 | 0.6 | -27.9 |
| Spiral 60° | 3.35 | 0.55 | -4.6 | -16.6 |
| Spiral 120° | 3.14 | 0.47 | -2.2 | -19.6 |

the contrast but reduces the lateral resolution.

CONCLUSION

A general improvement of the contrast was noted by using the spiral arrangement of the VS rather than a gridded one,

but both axial and lateral resolution are deteriorated. We assume that contrast improvement is linked to the diminution of grating lobes when using the spiral arrangement and the deterioration of resolution is due to the lower density of VS at the edges of the virtual probe.

In further studies it will be relevant to determinate the optimal number of VS which should be a trade-off between the resolution and contrast and the frame rate required for the considered application. The determination of an optimal VS location, using an optimization routine, may be realized in order to further compare the results with a deterministic way (regular and spiral distribution).

ACKNOWLEDGMENT

The Verasonics systems were co-funded by the FEDER program, Saint-EtienneMetropole (SME) and Conseil General de la Loire (CG42) within the framework of the SonoCardioProtection Project supervised by Prof. Pierre Croisille. The authors would also like to thank LabTAU for their contribution to the development of the 32 by 32 probe prototype compatible with driving 1 to 4 systems as well as for the provision of the

probe and two Vantage 256 systems and Labex Celya (ANR-10LABX-0060) for the funds that supported this research.

REFERENCES

- [1] R. W. Prager, U. Z. Ijaz, A. H. Gee and G. M. Treece, "Three-Dimensional Ultrasound Imaging", Proc. Inst. Mech. Eng. [H] 224, 193–223, 2010.
- [2] A. Fenster, D. B. Downey and H. N. Cardinal, "Three-Dimensional Ultrasound Imaging". Phys. Med. Biol. 46, R67 2001.
- [3] T. R. Nelson, and D. H. Pretorius, "Three-Dimensional Ultrasound Imaging", Ultrasound Med. Biol. 24, 1243–1270, 1998.
- [4] J. Provost, *et al.*, "3D Ultrafast Ultrasound Imaging *In Vivo*", Physics in Medicine and Biology, 59, L1, 10.1088/0031-9155/59/19/L1, 2014.
- [5] L. Sugeng *et al.*: "Quantitative Assessment of Left Ventricular Size and Function Side-by-Side Comparison of Real-Time Three-Dimensional Echocardiography and Computed Tomography With Magnetic Resonance Reference", Circulation 114, 654–661, 2006.
- [6] E. D. Light, S. F. Idriss, P. D. Wolf and S. W. Smith, "Real-time Three-Dimensional Intracardiac Echocardiography", Ultrasound Med. Biol. 27, 1177–1183, 2001.
- [7] G. D. Stetten *et al.*, "Real-time 3D Ultrasound: A New Look at the Heart", J. Cardiovasc. Diagn. Proced. 15, 73–84, 1998.
- [8] D. Garcia, P. Lantelme and É. Saloux, "Introduction to speckle tracking in cardiac ultrasound imaging", Handbook of speckle filtering and tracking in cardiovascular ultrasound imaging and video, (Loizou CP, Pattichis CS, d'Hooze J, ed.), Institution of Engineering and Technology, 2018.
- [9] D. Wildes *et al.*, "4-D ICE: A 2-D Array Transducer With Integrated ASIC in a 10-Fr Catheter for Real-Time 3-D Intracardiac Echocardiography", IEEE Trans. Ultrason. Ferroelectr. Freq. Control 63, 2159–2173, 2016.
- [10] P. Santos, G. U. Haugen, L. Løvstakken, E. Samset, and J. D'hooge, "Diverging Wave Volumetric Imaging Using Subaperture Beamforming", IEEE Trans. Ultrason. Ferroelectr. Freq. Control 63, 2114–2124, 2016.
- [11] G. Matrone *et al.*, "A volumetric CMUT-based ultrasound imaging system simulator with integrated reception and micro-beamforming electronics models", IEEE Trans. Ultrason. Ferroelectr. Freq. Control 61, 792–804, 2014.
- [12] A. Bhuyan *et al.*, "Integrated circuits for volumetric ultrasound imaging with 2-D CMUT arrays", IEEE Trans. Biomed. Circuits Syst. 7, 796–804, 2013.
- [13] J. Kortbek, J. A. Jensen and K. L. Gammelmark, "Sequential beamforming for synthetic aperture imaging", Ultrasonics 53, 1–16, 2013.
- [14] R. Fisher *et al.*, "Reconfigurable arrays for portable ultrasound, In Proc. IEEE Ultrason. Symp 1, 495–499, 2005.
- [15] I.O Wygant *et al.*, "An integrated circuit with transmit beamforming flip-chip bonded to a 2-D CMUT array for 3-D ultrasound imaging", IEEE Trans. Ultrason. Ferroelectr. Freq. Control 56, 2145–2156, 2009.
- [16] S. W. Smith, J. H. G. Pavy, and O. T. von Ramm, "High-speed ultrasound volumetric imaging system. I", Transducer design and beam steering. IEEE Trans. Ultrason. Ferroelectr. Freq. Control 38, 100–108, 1991.
- [17] O. T. von Ramm, S. W. Smith and J. H. G. Pavy, "High-speed ultrasound volumetric imaging system. II", Parallel processing and image display. IEEE Trans. Ultrason. Ferroelectr. Freq. Control 38, 109–115, 1991.
- [18] I. Ben Daya, A. Chen, M. J. Shafiee, A. Wong and J. T. W. Yeow, "Compensated Row-Column Ultrasound Imaging System Using Multilayered Edge Guided Stochastically Fully Connected Random Fields", Sci. Rep. 7, 2017.
- [19] H. Bouzari *et al.*, "Curvilinear 3-D Imaging Using Row-Column-Addressed 2-D Arrays With a Diverging Lens: Feasibility Study", IEEE Trans. Ultrason. Ferroelectr. Freq. Control 64, 978–988, 2017.
- [20] M. Flesch *et al.*, "4D in vivo ultrafast ultrasound imaging, using a row-column addressed matrix and coherently-compounded orthogonal plane waves" Phys. Med. Biol. 62, 4571, 2017.
- [21] T. L. Christiansen *et al.*, "3-D imaging using row-column-addressed arrays with integrated apodization - part ii: transducer fabrication and experimental results", IEEE Trans. Ultrason. Ferroelectr. Freq. Control 62, 959–971, 2015.
- [22] A. S. Logan, L. L. P. Wong, A. I. H. Chen and J. T. W. Yeow, "A 32 x 32 element row-column addressed capacitive micromachined ultrasonic transducer", IEEE Trans. Ultrason. Ferroelectr. Freq. Control 58, 1266–1271, 2011.
- [23] A. Savoia *et al.*, "P2B-4 Crisscross 2D cMUT Array: Beamforming Strategy and Synthetic 3D Imaging Results", IEEE Ultrasonics Symposium Proceedings 1514–1517, 2007.
- [24] B. Savord and R. Solomon, "Fully sampled matrix transducer for real time 3D ultrasonic imaging", IEEE Symposium on Ultrasonics 1, 945–953 Vol.1, 2003.
- [25] E. Roux, A. Ramalli, P. Tortoli, C. Cachard, Christian M. Robini and H. Liebgott, "2D Ultrasound Sparse Arrays Multi-Depth Radiation Optimization Using Simulated Annealing and Spiral-Array Inspired Energy Functions". IEEE Transactions on Ultrasonics, Ferroelectrics, and Frequency Control. 63. 2138-2149. 2016.
- [26] B. Diarra, M. Robini, P. Tortoli, C. Cachard and H. Liebgott, "Design of Optimal 2-D Nongrid Sparse Arrays for Medical Ultrasound", IEEE Trans. Biomed. Eng. 60, 3093–3102, 2013.
- [27] C. Tekes, M. Karaman and F. L. Degertekin, "Optimizing circular ring arrays for forward-looking IVUS imaging", IEEE Trans. Ultrason. Ferroelectr. Freq. Control 58, 2596–2607, 2011.
- [28] M. Karaman, I. O. Wygant, O. Oralkan and B. T. Khuri-Yakub, "Minimally Redundant 2-D Array Designs for 3-D Medical Ultrasound Imaging", IEEE Trans. Med. Imaging 28, 1051–1061, 2009.
- [29] A. Austeng and S. Holm, "Sparse 2-D arrays for 3-D phased array imaging - design methods", IEEE Trans. Ultrason. Ferroelectr. Freq. Control 49, 1073–1086, 2002.
- [30] A. Trucco, "Thinning and weighting of large planar arrays by simulated annealing", IEEE Trans. Ultrason. Ferroelectr. Freq. Control 46, 347–355, 1999.
- [31] E. Roux, A. Ramalli, H. Liebgott, C. Cachard, M. Robini and P. Tortoli. "Wideband 2-D Array Design Optimization With Fabrication Constraints for 3-D US Imaging", IEEE Transactions on Ultrasonics, Ferroelectrics, and Frequency Control, 64, 108-125, 2017.
- [32] E. Roux, F. Varray, L. Petrusca, C. Cachard, P. Tortoli, and H. Liebgott, "Experimental 3-D Ultrasound Imaging with 2-D Sparse Arrays using Focused and Diverging Waves", Scientific Reports, vol. 8, no. 1, Dec. 2018.
- [33] E. Roux, "2D sparse array optimization and operating strategy for real-time 3D ultrasound imaging", PhD thesis, Université de Lyon, 2016.
- [34] L. Petrusca *et al.* "Fast Volumetric Ultrasound B-Mode and Doppler Imaging with a New High-Channels Density Platform for Advanced 4D Cardiac Imaging/Therapy", Appl. Sci. 8, 200, 2018.
- [35] G. Montaldo, M. Tanter, J. Bercoff, N. Benceh, and M. Fink, "Coherent plane-wave Compounding for very high frame rate ultrasonography and transient elastography", IEEE Transactions on Ultrasonics, Ferroelectrics, and Frequency Control, vol. 56, no. 3, pp. 489–506, Mar. 2009.